Radiance transmittance measured at the ocean surface

Jianwei Wei,[1,*] Zhongping Lee,[1] Marlon Lewis,[2] Nima Pahlevan,[3,4] Michael Ondrusek,[5] and Roy Armstrong[6]

[1] *Optical Oceanography Laboratory, School for the Environment, University of Massachusetts Boston, Boston, MA 02125, USA*

[2] *Department of Oceanography, Dalhousie University, Halifax, NS, B3H 4J1, Canada*

[3] *NASA Goddard Space Flight Center, Terrestrial Information Systems Laboratory, Greenbelt, MD 20771, USA*

[4] *Science, Systems and Applications, Inc (SSAI), Lanham, MD 20706, USA*

[5] *NOAA Center for Weather and Climate Prediction (NCWCP), College Park, MD 20740, USA*

[6] *Bio-optical Oceanography Laboratory, University of Puerto Rico, Mayagüez, PR 00681, USA*

**jianwei.wei@umb.edu*

Abstract: The radiance transmittance (*Tr*) is the ratio of the water-leaving radiance ($L_w(0^+)$) to the sub-surface upwelling radiance ($L_u(0^-)$), which is an important optical parameter for ocean optics and ocean color remote sensing. Historically, a constant value (~0.54) based on theoretical presumptions has been adopted for *Tr* and is widely used. This optical parameter, however, has never been measured in the aquatic environments. With a robust setup to measure both $L_u(0^-)$ and $L_w(0^+)$ simultaneously in the field, this study presents *Tr* in the zenith direction between 350 and 700 nm measured in a wide range of oceanic waters. It is found that the measured *Tr* values are generally consistent with the long-standing theoretical value of 0.54, with mean relative difference less than 10%. In particular, the agreement within the spectral domain of 400-600 nm is found to be the best (with the averaged difference less than 5%). The largest difference is observed for wavelengths longer than 600 nm with the average difference less than 15%, which is related to the generally very small values in both $L_u(0^-)$ and $L_w(0^+)$ and rough environmental conditions. These results provide a validation of the setup for simultaneous measurements of upwelling radiance and water-leaving radiance and confidence in the theoretical *Tr* value used in ocean optics studies at least for oceanic waters.

OCIS codes: (010.0010) Atmospheric and oceanic optics; (010.4450) Oceanic optics; (120.0280) Remote sensing and sensors; (010.5620) Radiative transfer.

References and links

1. H. R. Gordon and A. Morel, *Remote Assessment of Ocean Color for Interpretation of Satellite Visible Imagery: A Review* (Springer-Verlag, 1983).
2. C. D. Mobley, *Light and Water: Radiative Transfer in Natural Waters* (Academic Press, 1994).
3. R. W. Austin, "Inherent spectral radiance signatures of the ocean surface," in *Ocean Color Analysis*, S. Q. Duntley, R. W. Austin, W. H. Wilson, C. F. Edgerton, and S. E. Moran, eds. (Scripps Institution of Oceanography, 1974), pp. 2–1 - 2–20.
4. F. E. Nicodemus, "Radiance," Am. J. Phys. **31**(5), 368–377 (1963).
5. R. W. Preisendorfer, *Hydrologic Optics* (U.S. Government Printing Office, 1976).
6. R. W. Austin, "The remote sensing of spectral radiance from below the ocean surface," in *Optical Aspects of Oceanography*, N. G. Jerlov and E. Steemann Nielsen, eds. (Academic Press, 1974), pp. 317–344.
7. R. W. Austin, "Gulf of Mexico, ocean-color surface-truth measurements," Bound. Lay. Meteorol. **18**(3), 269–285 (1980).
8. A. Morel, "In-water and remote measurements of ocean color," Bound. Lay. Meteorol. **18**(2), 177–201 (1980).
9. H. R. Gordon, O. B. Brown, R. H. Evans, J. W. Brown, R. C. Smith, K. S. Baker, and D. K. Clark, "A semianalytic radiance model of ocean color," J. Geophys. Res. **93**(D9), 10909–10924 (1988).
10. Z. Lee, K. L. Carder, C. D. Mobley, R. G. Steward, and J. S. Patch, "Hyperspectral remote sensing for shallow waters. I. A semianalytical model," Appl. Opt. **37**(27), 6329–6338 (1998).

#234268 - $15.00 USD Received 10 Feb 2015; revised 3 Apr 2015; accepted 23 Apr 2015; published 27 Apr 2015

11. A. Morel and B. Gentili, "Diffuse reflectance of oceanic waters. II Bidirectional aspects," Appl. Opt. **32**(33), 6864–6879 (1993).
12. G. Zibordi, K. Ruddick, I. Ansko, G. Moore, S. Kratzer, J. Icely, and A. Reinart, "In situ determination of the remote sensing reflectance: an inter-comparison," Ocean Sci. **8**(4), 567–586 (2012).
13. Z. Lee, N. Pahlevan, Y.-H. Ahn, S. Greb, and D. O'Donnell, "Robust approach to directly measuring water-leaving radiance in the field," Appl. Opt. **52**(8), 1693–1701 (2013).
14. K. J. Voss, S. McLean, M. R. Lewis, C. Johnson, S. Flora, M. Feinholz, M. Yarbrough, C. C. Trees, M. S. Twardowski, and D. K. Clark, "An example crossover experiment for testing new vicarious calibration techniques for satellite ocean color radiometry," J. Atmos. Ocean. Technol. **27**(10), 1747–1759 (2010).
15. R. Leathers, T. Downes, and C. Mobley, "Self-shading correction for oceanographic upwelling radiometers," Opt. Express **12**(20), 4709–4718 (2004).
16. Z. P. Lee, C. Hu, S. Shang, K. Du, M. Lewis, R. Arnone, and R. Brewin, "Penetration of UV-visible solar radiation in the global oceans: insights from ocean color remote sensing," J. Geophys. Res. **118**, 1–15 (2013).
17. Z. P. Lee, "Update of the quasi-analytical algorithm (QAA_v6)" (2014), retrieved *http://www.ioccg.org/groups/Software_OCA/QAA_v6_2014209.pdf*.
18. H. R. Gordon and K. Ding, "Self-shading of in-water optical instruments," Limnol. Oceanogr. **37**(3), 491–500 (1992).
19. G. Zibordi and G. M. Ferrari, "Instrument self-shading in underwater optical measurements: experimental data," Appl. Opt. **34**(15), 2750–2754 (1995).
20. J. L. Mueller, G. S. Fargion, and C. R. McClain, eds., *Ocean Optics Protocols for Satellite Ocean Color Sensor Validation, Revision 4* (NASA, Goddard Space Flight Center, Greenbelt, MD, 2003), Vol. III, pp. 78.
21. W. W. Gregg and K. L. Carder, "A simple spectral solar irradiance model for cloudless maritime atmospheres," Limnol. Oceanogr. **35**(8), 1657–1675 (1990).
22. H. R. Gordon, "Contribution of Raman scattering to water-leaving radiance: a reexamination," Appl. Opt. **38**(15), 3166–3174 (1999).
23. J. Wei, M. R. Lewis, R. Van Dommelen, C. J. Zappa, and M. S. Twardowski, "Wave-induced light field fluctuations in measured irradiance depth profiles: A wavelet analysis," J. Geophys. Res. **119**(2), 1344–1364 (2014).

1. Introduction

The water-leaving radiance right above the water surface ($L_w(0^+)$, unit: μW cm^{-2} sr^{-1} nm^{-1}) is the fundamental radiometric quantity for ocean color remote sensing. Originating from the upwelling radiance right below the water surface ($L_u(0^-)$, unit: μW cm^{-2} sr^{-1} nm^{-1}), the water-leaving radiance carries important information about the water constituents present in the surface layers of the ocean [1]. Following radiative transfer, $L_w(0^+)$ is the resultant radiance of $L_u(0^-)$ after the cross-surface transmission [2],

$$L_w(0^+) = Tr \cdot L_u(0^-) \tag{1}$$

where Tr is the radiance transmittance (dimensionless). The value of this transmittance was determined as a constant Tr = 0.54 [3], primarily based on assumptions of the relative refractive index of water. This theoretical constant has ever since been widely adopted by the optical oceanography community.

The upwelling radiance transmission across the air-water interface follows the "radiance n^2 law" [4, 5], by which the transmittance can be specifically expressed as [3, 6],

$$Tr = \frac{1-\rho}{n_w^{\,2}} \tag{2}$$

In this model n_w is the refractive index of the bulk seawater and ρ is the sea surface reflectance from below; the wavelength dependence is suppressed for brevity. The two quantities ρ and n_w are usually treated as constants (ρ = 0.025 for the nadir-viewing radiance, and n_w = 1.34) [3, 6–8], henceforth leading to a constant transmittance. For ocean optics studies or processing satellite ocean color data, it is required to know the value of Tr in order to convert $L_w(0^+)$ to $L_u(0^-)$ or vice versa [9–12]. Although a theoretical value has been assigned to Tr [3, 7, 8], there have been no direct measurements in the field to verify this bulk water property.

#234268 - $15.00 USD Received 10 Feb 2015; revised 3 Apr 2015; accepted 23 Apr 2015; published 27 Apr 2015

The objective of this study is henceforth to assess the optical closure of the upwelling radiance transmission in a wide range of ocean waters and to test the hypothesis that the radiance transmittance factor is a constant with a magnitude of 0.54. The work is based on direct observations in a wide range of ocean environments using novel instrumentation for collocated measurement of the upwelling nadir radiance and water-leaving radiance.

2. Data and methods

2.1 Locations of measurements

Field measurements were carried out in five optically different ocean waters [see Fig. 1]. Three stations were measured in the northern Gulf of Mexico (GM) in September 2013 where the water color is generally light blue. In November 2013, two stations were measured in Massachusetts Bay (Mass), about 15 miles east of the Boston harbor. This region is characterized by green water color. The third location was at the Aqua Alta oceanographic tower (AAOT) in the Adriatic Sea (Adri), off the Venice Lagoon, Italy. The water exhibited milky green to turquoise blue color. The fourth location was in the Northwest Atlantic (NWA), east of South Carolina, in November 2014 where three stations were measured with water color dark blue. The fifth location was in the blue waters in the Caribbean Sea (Cari), south of Puerto Rico on December 13, 2014. Among all stations, the NWA represents the clearest waters with chlorophyll a concentration of 0.24-0.55 mg m^{-3}.

All experiments were completed in optically deep waters with a variety of atmospheric conditions and sea states. Both clear skies and cloudy skies were encountered, with the solar zenith angle ranging from 25° to 70° and the wave heights from 0.25 m to 2.5 m (Table 1), respectively.

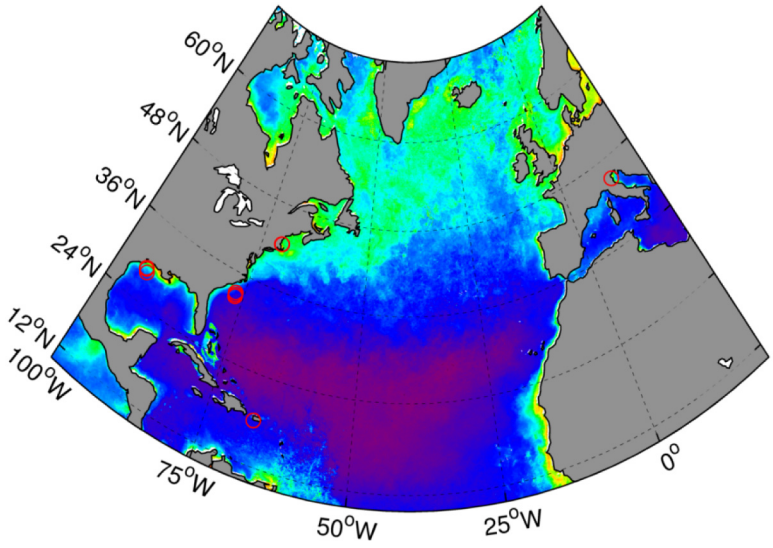

Fig. 1. Field experiment stations overlaid on a yearly chlorophyll a distribution map (SeaWiFS level-3 yearly chlorophyll a concentration map for 2010).

#234268 - $15.00 USD Received 10 Feb 2015; revised 3 Apr 2015; accepted 23 Apr 2015; published 27 Apr 2015

Table 1. Environmental conditions during the field transmittance measurements.

Experiment sites	Sta. #	Date	Latitude /Longitude	Water depth (m)	Solar zenith (°)	Wave height (m)	Sky condition
Gulf of Mexico	54	Sept-15-2013	28.196°, –93.798°	69	56	2.5	variable
	57		28.573°, –94.118°	35	41	2.5	variable
	58		28.701°, –94.242°	30	69	2.5	variable
Massachusetts Bay	11	Nov-16-2013	42.413°, –70.458°	40	61	0.27	opaque
	10		42.405°, –70.547°	50	64	0.25	sunny
Adriatic Sea, Italy	3	Jun-24-2014	45.317°, 12.500°	30	26	0.48	variable
	5	Jun-26-2014	45.317°, 12.508°	30	35	0.38	variable
Northwest Atlantic Ocean	4	Nov-13-2014	32.626°, –76.643°	943	69	~1	sunny
	5		32.868°, –76.744°	702	51	1.5	sunny
	6		33.154°, –76.814°	473	60	~1	opaque
Caribbean Sea	1	Dec-13-2014	17.862°, –66.973°	1000	41	1.5	opaque
	2		17.907°, –66.972°	600	41	1.5	Sunny

2.2 Instrumental setup for collocated radiance measurements

To accurately determine the radiance transmittance, it is required to measure $L_w(0^+)$ and $L_u(0^-)$ simultaneously. $L_u(0^-)$ is commonly obtained from an in-water radiometer, but it is not easy to obtain $L_w(0^+)$ experimentally. To minimize the impact of surface-reflected skylight on the determination of $L_w(0^+)$, the skylight-blocked approach (SBA) [13] was adopted to obtain "true" $L_w(0^+)$ in the field.

Two hyperspectral ocean color radiometers (HyperOCR, Satlantic Inc, Canada) were configured to measure the water-leaving radiance ($L_w(0^+)$) and in-water upwelling radiance ($L_u(z)$), respectively. The HyperOCR sensors are fully digital optical packages. They have a field of view (FOV) of 3° in air (8.5° in water). The radiance can be measured at ~3 nm increments from the ultraviolet (UV) to near-infrared (NIR) bands with a wavelength accuracy of ± 0.1 nm. Each spectral band is approximately 10 nm wide. All instruments were calibrated by reference to standard products by the National Institute of Standards and Technology (NIST). The measurement uncertainties for the radiance instrument are reportedly less than 2.8% [14].

The two radiance radiometers were placed on the two fins of a hyperspectral profiler (HyperPro) [Fig. 2] with each arm about 30 cm long. Both sensors looked downward and recorded the radiance at almost the same time (time difference is usually less than 0.5 s), with a sampling frequency ~1Hz. The profiler was configured to float at the sea surface. With this setup, one radiometer measured L_w while the other one measured $L_u(z)$. For the measurement of $L_w(0^+)$, a customized cone was attached to the HyperOCR L_w radiometer (s/n: HPL343) (housing diameter ~6 cm) with its open end (10 cm in diameter) immersed just below the water surface, while the radiometer window remains in the air, such that the surface-reflected light is blocked off the field of view of the radiometer (see [13] for details). The upwelling radiance ($L_u(z)$) below water surface (a nominal depth of ~15 cm) was measured with the

#234268 - $15.00 USD Received 10 Feb 2015; revised 3 Apr 2015; accepted 23 Apr 2015; published 27 Apr 2015

second HyperOCR radiometer (s/n: HPL191 and HPL372; HPL191 was used in the Gulf of Mexico and Massachusetts Bay, while HPL372 was deployed in the Adriatic Sea and West Atlantic Ocean).

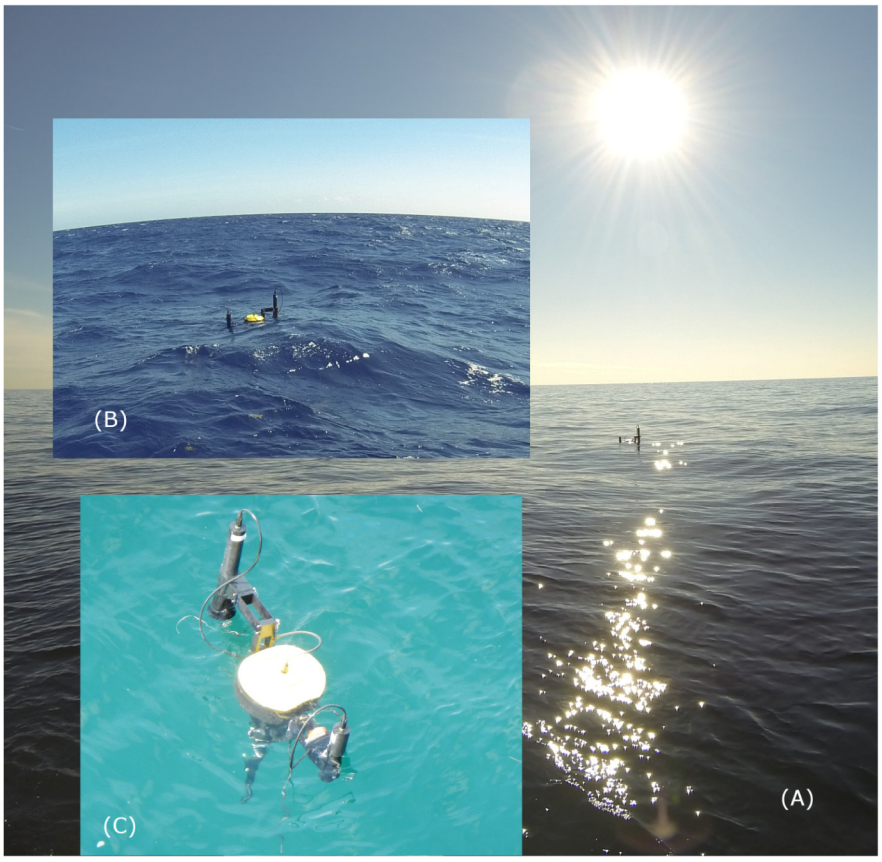

Fig. 2. Collocated observation of the water-leaving radiance using the skylight-blocked approach (SBA) and the upwelling radiance. The background image (A) was taken on November 16, 2013, in Massachusetts Bay. The inserted image (B) was taken in the Caribbean Sea, south of Puerto Rico on December 13, 2014. Image (C) was captured in the Adriatic Sea, off the Venice Lagoon, Italy, on June 24, 2014. As shown in (C), the L_w sensor (on the left wing) is suspended in the air while the skylight is blocked off by the cone, and the L_u sensor (attached on the right wing) is completely immersed into water.

During the field deployments, this instrument package was kept at least 20 meters away from the vessel in order to minimize the shadowing effect of the ship, or reflections from the hull. Moreover, the instrument package was maneuvered so that the orientation of the L_w and L_u sensors was perpendicular to the plane of the Sun beam, therefore maintaining same incident light for both sensors.

Additional comparisons of the instruments accuracies were carried out right before or after the field experiments. The first test was made in August 2013, when the two radiance sensors (HPL 343 and HPL191) were put side by side to simultaneously measure the reflected solar radiation from a standard gray card (18% reflectance). The second test was implemented right before the field observations in the Adriatic Sea and the Northwest Atlantic Ocean in the lab by measuring the standard light source of a FEL lamp as reflected from a Spectralon® calibrated reflectance standard. These tests indicated that consistent measurements of radiance (± 5%) by both sensors. This performance measure is independent of the calibration

#234268 - $15.00 USD Received 10 Feb 2015; revised 3 Apr 2015; accepted 23 Apr 2015; published 27 Apr 2015

of the radiometers. The manufacturer's radiometric calibration (and the immersion factor for the in-water sensors) was applied for subsequent data analyses.

2.3 Characterization of the water bodies

To characterize the water optical properties and as well to derive the attenuation coefficient required to propagate L_u(depth z = 0.15 m) to $L_u(0^-)$, the remote sensing reflectance (R_{rs}, units: sr^{-1}, which is the ratio of $L_w(0^+)$ to downwelling irradiance just above the surface) was measured with the SBA scheme [13] at each station. The instrument package was deployed >20 m away from the ship to avoid the shadow or reflection of the hull. For the measured above-water downwelling irradiance (E_s, unit: $\mu W cm^{-2} nm^{-1}$) and $L_w(0^+)$ data pairs, only those data where the package inclination was less than 5° were used for further analysis. The E_s was interpolated spectrally so as to match up with the wavelengths of the L_w sensor. The instantaneous remote sensing reflectance was first determined as the ratio of instantaneous $L_w(0^+)$ to E_s

$$R_{rs}(\lambda,t) = \frac{L_w(0^+,\lambda,t)}{E_s(\lambda,t)} \tag{3}$$

The determination of remote sensing reflectance $R_{rs}(\lambda)$ were further carried out by filtering out the data frames for which the remote sensing reflectance at 698 nm falls outside of ± 30% of the first mode of the density function of all available data sequence of $R_{rs}(698,t)$. This procedure effectively eliminated those potentially contaminated measurements with sea surface reflection and/or immersed sensor head at high sea conditions. Usually more than 1/3 of the measurements were remained after the above filtering. The remaining $R_{rs}(\lambda,t)$ data were then used to derive the median spectra, and this median was taken as the $R_{rs}(\lambda)$ of the measurement station.

The measured R_{rs} spectra represented a wide range of ocean waters, with $R_{rs}(400)$ varying by a factor of 9 [Fig. 3(a)]. Five stations can be characterized as green waters, including Massachusetts Bay, the Adriatic Sea and one station in the Gulf of Mexico. The other stations are all typical clear blue oceanic waters with high reflectance at shorter wavelengths and very low values in the red part of the spectra.

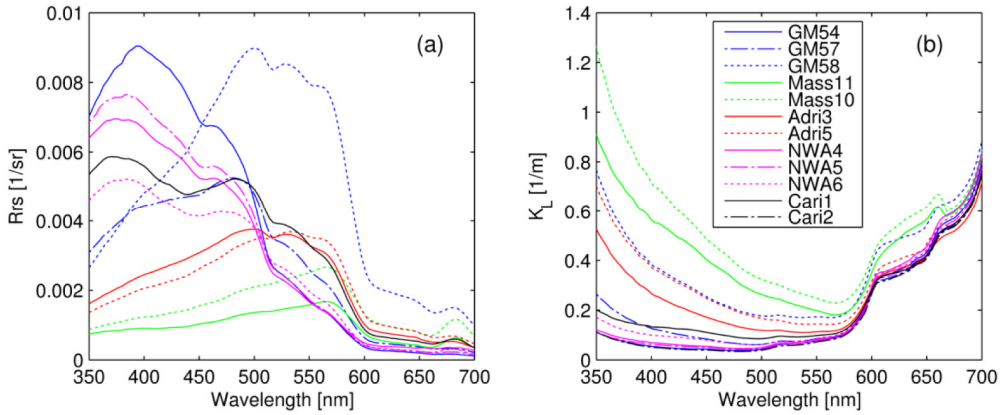

Fig. 3. (a) Measured remote sensing reflectance and (b) estimated diffuse attenuation coefficient. The Arabic numbers after the abbreviations refer to the station numbers.

#234268 - $15.00 USD Received 10 Feb 2015; revised 3 Apr 2015; accepted 23 Apr 2015; published 27 Apr 2015

2.4 Data reduction for collocated radiance measurements

2.4.1 Radiance data pre-processing

The radiometric data were first processed following the manufacturer's radiometric data processing protocols (referred to as Level-2). First, dark values were taken every five samples by use of an internal shutter. These measurements were linearly interpolated for each light measurement, and then subtracted from the observations. The calibration coefficients provided by the manufacturer were used to convert the raw data to radiometric units of μW cm^{-2} sr^{-2} nm^{-1}. The immersion factor (I_f) was only applied to the L_u measurements. For the L_w sensor, which was configured to operate in air, no immersion effect was considered in the data processing. Spectral interpolation was applied to the measured L_u data in order to match the wavelengths of L_w data. Note that the two hyperspectral radiometers did not sample at exactly the same time, but generally were recorded within 0.5 second (for 90% of the measurement sequence).

2.4.2 Derivation of subsurface upwelling radiance $L_u(0^-)$

Since the upwelling radiance was measured at a depth of ~0.15 m, it is necessary to propagate it from this depth to right below the water surface ($z = 0^-$ m) to obtain $L_u(0^-)$. To do so, the exponential decay relationship [15] was assumed for the $L_u(z)$ depth profile in the surface layer, thus $L_u(0^-) = L_u(z)\cdot\exp(K_L\cdot 0.15)$, where K_L (unit: m^{-1}) is the diffuse attenuation coefficient for the upwelling nadir radiance. In this study, the diffuse attenuation coefficient for the downwelling irradiance (K_d, unit: m^{-1}) was first estimated with the model of Lee, et al. [16], which can be approximated as K_L (Lin and Lee, manuscript in preparation). The semi-analytical model requires knowledge of the total absorption coefficient $a(\lambda)$ and backscattering coefficient $b_b(\lambda)$. We estimated $a(\lambda)$ and $b_b(\lambda)$ using the latest quasi-analytical algorithm (QAA, version 6) [17]. It is emphasized that the effects of errors in the estimated K_d or K_L on the extrapolated $L_u(0^-)$ are limited because the propagation depth for $L_u(z)$ to $L_u(0^-)$ is only 0.15 m.

The diffuse attenuation coefficients are illustrated in Fig. 3(b). The greenish waters in the Massachusetts Bay and Adriatic Sea are the most turbid ($K_d(440)$ ~0.5 m^{-1}) among all 12 stations and their K_d's therein are distinctively different from the blue waters in both their magnitudes and spectral shapes. Maximum K_d's are often observed at both the shorter and longer ends of the spectrum. The blue waters are characterized by high diffuse attenuation coefficients at the red end. Based on these spectral K_d values, the $L_u(0^-)$ can be increased by up to 10% at 380 nm and 16% at 670 nm relative to $L_u(0.15)$.

2.4.3 Instrument self-shading correction

Because both radiance sensors are more or less in the way of illumination from the Sun and the sky, inevitably there is self-shading effect on the collected $L_w(0^+)$ and $L_u(0.15)$ data, which need to be corrected for the calculation of T_r and R_{rs}. We used the model of Gordon and Ding [18] for this correction, which is validated by field observations [19]. According to the recommended practice [20], a key parameter required for the correction is the diameter of the instrument. The diameter of the cone (D = 0.1 m) was used for self-shading correction of $L_w(0^+)$ data, while the diameter of the radiometer housing (D = 0.06 m) was used for the correction of L_u data.

Application of the correction requires the spectral ratio of the diffuse irradiance to direct irradiance [18]. For sunny and variable skies, the ratio was estimated from the RADTRAN model [21]. For the opaque skies, no shade-correction was applied to the radiance measurements.

#234268 - $15.00 USD Received 10 Feb 2015; revised 3 Apr 2015; accepted 23 Apr 2015; published 27 Apr 2015

2.4.4 Filtering of $L_w(0^+)$ and $L_u(0^-)$ data

The obtained $L_w(0^+)$ and $L_u(0^-)$ data sequences were subject to further quality-controls. First, the measurements with instrument inclination greater than 5° were removed from the subsequent analyses. Three situations were further taken into account in the data filtering. First, it was observed that the cone attached to the L_w instrument could be occasionally popped out of the water surface at high seas. Data collected at those moments could be contaminated by the surface-reflected skylight. In addition, under certain circumstances, the L_w sensor head could be immersed into the water with passing-by waves. Further, because the above-water irradiance could change with moving clouds (Table 1), the consequent $L_w(0^+)$ and $L_u(0^-)$ values thus would also change. To reduce the uncertainties in the transmittance due to such natural variations, we derived the instantaneous transmittance as the ratio of $L_w(0^+)$ to $L_u(0^-)$,

$$Tr(\lambda)^i = \frac{L_w(0^+,\lambda)^i}{L_u(0^-,\lambda)^i} \tag{4}$$

where the superscript i stands for the i^{th} radiance pairs in the available radiance data sequence after previous quality-control steps. Similar to the R_{rs} data processing, the mode of $Tr(698)^i$ sequence was then determined from its density function. The $Tr(\lambda)^i$ spectra were filtered out from the data sequences if the observed $Tr(698)^i$ exceeded the mode by ± 30%. This filtering step removed <30% of the data. The transmittance spectrum was then determined as the median of the remaining $Tr(\lambda)^i$ spectra. With the above quality control, the resultant $L_w(0^+)$ and $L_u(0^-)$ data sets exhibit small variability with the coefficient of variation (defined as the ratio of the standard deviation to the median value of radiance data) generally less than 15% at 350-700 nm range, except for occasional larger variability (Table 2).

Table 2. Coefficient of variation (× 100%) for water-leaving radiance $L_w(0^+)$ and $L_u(0^-)$ (within the parentheses).

	Sta.#	Wavelength (nm)					
		380	412	443	490	555	670
Gulf of Mexico	54	0.11(0.05)	0.10(0.05)	0.10(0.05)	0.10(0.05)	0.14(0.09)	0.42(0.26)
	57	0.11(0.07)	0.11(0.07)	0.11(0.07)	0.11(0.07)	0.11(0.07)	0.11(0.09)
	58	0.10(0.10)	0.10(0.10)	0.10(0.10)	0.10(0.10)	0.11(0.11)	0.16(0.17)
Massachu-setts Bay	11	0.12(0.02)	0.10(0.03)	0.08(0.03)	0.06(0.03)	0.05(0.03)	0.10(0.03)
	10	0.03(0.03)	0.04(0.03)	0.03(0.03)	0.03(0.02)	0.02(0.02)	0.08(0.04)
Adriatic Sea, Italy	3	0.05(0.05)	0.05(0.05)	0.05(0.05)	0.05(0.05)	0.06(0.06)	0.08(0.07)
	5	0.11(0.10)	0.12(0.12)	0.13(0.13)	0.14(0.13)	0.15(0.14)	0.16(0.13)
Northwest Atlantic Ocean	4	0.03(0.03)	0.03(0.04)	0.03(0.04)	0.04(0.05)	0.04(0.05)	0.03(0.02)
	5	0.08(0.07)	0.09(0.08)	0.10(0.09)	0.09(0.09)	0.09(0.09)	0.05(0.04)
	6	0.03(0.02)	0.03(0.02)	0.04(0.03)	0.05(0.03)	0.05(0.03)	0.07(0.01)
Caribbean Sea	1	0.23(0.22)	0.27(0.26)	0.29(0.29)	0.31(0.30)	0.33(0.32)	0.22(0.22)
	2	0.05(0.03)	0.05(0.04)	0.05(0.04)	0.05(0.04)	0.05(0.05)	0.06(0.02)

#234268 - $15.00 USD Received 10 Feb 2015; revised 3 Apr 2015; accepted 23 Apr 2015; published 27 Apr 2015

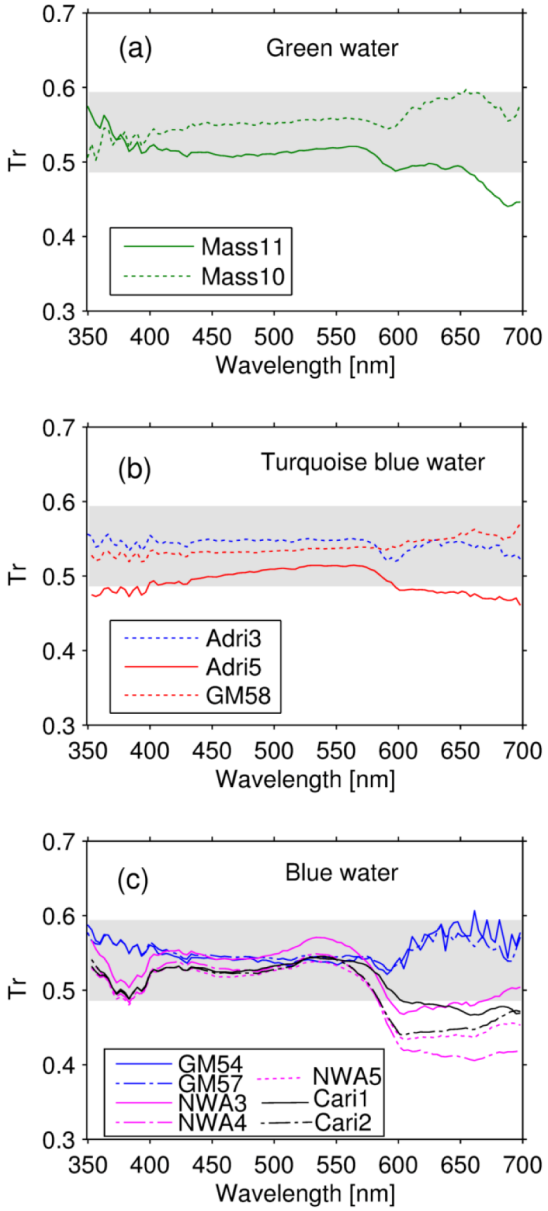

Fig. 4. Spectral radiance transmittance obtained in various ocean waters. The shaded area represents the domain of ± 10% deviation from the theoretical transmittance Tr = 0.54.

3. Results

In the green ocean waters of the Massachusetts Bay [Fig. 4(a)], the in situ measured transmittance is generally within ± 10% of the theoretical prediction (calculated as $\delta = (Tr\text{-}0.54)/0.54 \times 100\%$) between 350 nm and 700 nm. At the red end of spectrum, slightly larger deviations (beyond 10%) are seen from the theoretical constant but are still within ± 20%.

In the turquoise waters including the stations in the Adriatic Sea and one station in the Gulf of Mexico [Fig. 4(b)], the best model-data agreement (with relative error within ± 10%) is achieved for spectral bands between 400 nm and 600 nm. Similar to the green waters, relatively larger deviations are occasionally found at the red bands as well as the UV bands,

#234268 - $15.00 USD Received 10 Feb 2015; revised 3 Apr 2015; accepted 23 Apr 2015; published 27 Apr 2015

which are however still within ± 20%. There is no sign of significant spectral dependence of the mean transmittance.

For the blue water measurements in Fig. 4(c), including two stations in the Gulf of Mexico, and all stations in the Northwest Atlantic and Caribbean Sea, good model-data agreement is found for the wavelengths of 350-600 nm (relative differences within ± 10%). In the red bands between 600 nm and 700 nm, the measured transmittance shows systematic underestimation relative to the theoretical transmittance (beyond −10%), except for measurements in the Gulf of Mexico. In particular, the model-data discrepancy exceeds 20% for the wavelengths between 600 and 700 nm in the Northwest Atlantic Ocean and Caribbean Sea. In part, this could be related to the small values of the radiance at longer wavelengths in the blue waters where both $L_w(0^+)$ and $L_u(0^-)$ are close to zero and small (absolute) differences in radiance measurements can transfer to large errors in the transmittance.

The relative percentage difference, δ, between the derived transmittance and theoretical transmittance was averaged for the green, turquoise, and blue ocean waters, respectively, and presented in Table 3. On average, the model-data difference is generally within 5% from the UV bands through the green bands, and increases for red band transmittance in blue oceanic waters, where the percentage difference reaches up to 13%, likely in part due to the extremely small $L_w(0^+)$ and $L_u(0^-)$ values.

The measurement uncertainty of transmittance is further quantified by its coefficient of variation (ratio of the standard deviation to the median value) and presented in Fig. 5. The least uncertainty is observed at green wavelength (mostly less than 5%), moderate uncertainty is with the shorter wavelengths (less than 10%), and the largest uncertainty is usually at red bands (generally less than 20%). The spectral dependence of the uncertainty of the measured *Tr* is related to the variability of $L_w(0^+)$ and $L_u(0^-)$ shown in Table 2, which are in principle caused by the varying intensities of both radiance at different wavelengths.

Another conclusion, which may be drawn from Fig. 5, is that the uncertainty of the measured *Tr* is likely related to the sky conditions: measurements made under sunny skies (stations of Mass11, NWA4, NWA5, Cari2) have shown small uncertainty (generally less than 5%); those with variable skies (at stations GM54, GM57, GM58, Adri3, Adri5, Mass11, NWA6 and Cari6) usually have relatively larger uncertainties at shorter and longer wavelengths.

Table 3. Mean absolute percentage difference (× 100%) between measured *Tr* and the theoretical value. The numbers in bold face denote the discrepancy exceeding 0.10.

Water types	Wavelength (nm)					
	380	412	443	490	555	670
Green waters	0.01	0.02	0.04	0.04	0.04	**0.11**
Turquoise waters	0.05	0.04	0.04	0.03	0.02	0.06
Blue waters	0.07	0.02	0.02	0.02	0.01	**0.13**

#234268 - $15.00 USD Received 10 Feb 2015; revised 3 Apr 2015; accepted 23 Apr 2015; published 27 Apr 2015

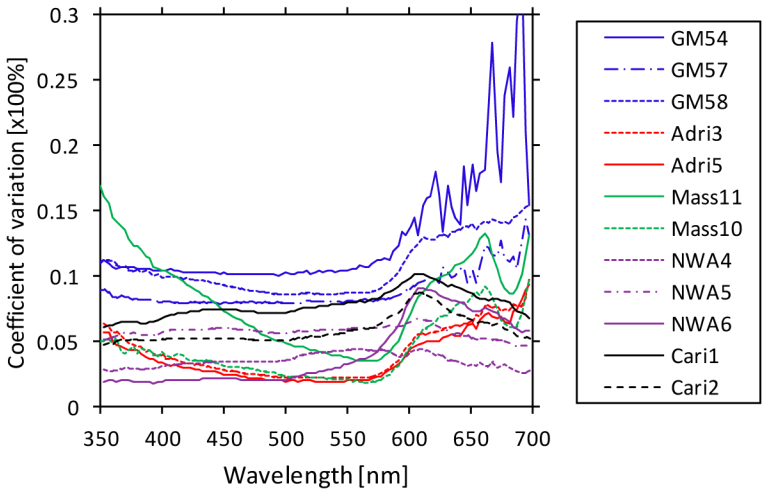

Fig. 5. Coefficient of variation for the measured radiance transmittance

4. Discussion

The theory-data agreement in the spectral bands of 400 - 600 nm is remarkable (with $\delta < 5\%$), particularly considering the fact that the water-leaving radiance $L_w(0^+)$ and the upwelling radiance $L_u(0^-)$ are in general extremely difficult to be measured accurately in the field [13]. This finding supports the general validity of a constant transmittance for the upwelling radiance [3] at these bands at least for oceanic waters. Apart from the theory-data consistency, relatively larger differences are found in the UV domain and red wavelengths, up to 7% and 13%, respectively (Table 3). The instrumentation, low intensities and the measurement conditions could be responsible for the larger variations at these wavelengths.

Assuming a true absorption coefficient, we estimated the effects of the instrumental self-shading correction on the radiance measurements and the consequent transmittance. Among all our measurements, the largest self-shading errors with radiance (still less than 15%) are usually observed at red bands where the absorption coefficient are generally high (data not shown here). In the UV, blue and green spectral domain, the self-shading error is generally less than 5%. However, the instrument self-shading effect contributes to the transmittance (the ratio of $L_w(0^+)$ to $L_u(0^-)$) by no more than 8% at red bands and less than 3% at other wavelengths. It is noted that the Gordon and Ding [18] self-shading model was developed for clear sky conditions, thus no self-shading correction was applied for measurements under variable cloud conditions. However, because Tr is the ratio of $L_w(0^+)$ to $L_u(0^-)$, and both sensors were subject to similar shading effects, thus the impact on Tr with no correction under such a condition should be limited.

Errors in the estimated K_L at longer wavelengths are likely limited because the diffuse attenuation coefficient therein is dominated by the absorption of pure seawater. Due to the short depth (0.15 m) used for the propagation of $L_u(z)$ to $L_u(0^-)$, the errors in K_L alone do not exert significant impact on $L_u(0^-)$. Assuming a true $K_L(\lambda)$ as 1.0 m^{-1} and the estimated K_L contains 20% error, for example, the estimated $L_u(0^-)$ will consequently be subjected to a 5% error for an ideal calm water surface (e.g., instrument is at the nominal depth of 0.15 m). These errors are even smaller at wavelengths from 400 nm to 600 nm because the magnitudes of the diffuse attenuation coefficient $K_L(\lambda)$ at these bands are small [Fig. 3(b)]. Further, the effect of estimated K_L on the $L_u(0^-)$ determination could be ignored at wavelengths less than 600 nm in clear oceanic waters (in our case, including Gulf of Mexico, Northwest Atlantic and Caribbean Sea), because the product of K_L and the sensor depth is minimal.

#234268 - $15.00 USD Received 10 Feb 2015; revised 3 Apr 2015; accepted 23 Apr 2015; published 27 Apr 2015

Raman scattering will contribute to upwelling radiance [22], especially in the longer wavelengths. Ignoring the Raman scattering may introduce some errors to K_L and consequently the estimated $L_u(0^-)$ from $L_u(z)$. But the impact is negligible because of the short propagating distance (0.15 m). Therefore the omission of Raman scattering has negligible effect on the calculation of cross-surface transmittance (Tr), at least for the wavelengths considered (see above).

The light field in surface water is spatially and temporally variable due to the wave focusing effect, with the most significant variability toward longer wavelengths [23]. The observed radiance variability in Table 2 is due in part to the focusing of waves and can be partly ascribed to the variability of above-water irradiance.

5. Conclusions

We examined the spectral transmittance of upwelling radiance based on collocated measurements of the upwelling radiance and water-leaving radiance. The measurements of a wide range of radiative and optical properties have provided a unique data set to verify for the first time the long-standing presumption about the constant radiance transmittance. In comparison with our measurements, the assumed radiance transmittance is found to be consistent with observations, with a mean percentage difference less than 5% over the wavelengths of 350-600 nm. Relatively larger deviations between the measurements and the theoretical value is found at red wavelengths (600-700 nm) with δ<15%, which can be attributed to the quite small radiance values at these wavelengths and in part to the vertical displacements of instrument in high sea states. This larger discrepancy emphasizes the importance and practical difficulty in obtaining accurate $L_u(0^-)$ and $L_w(0^+)$ at longer wavelengths and in high seas. Our measurements in the UV domain do not show large discrepancy relative to the theoretical transmittance, even in the green and turquoise ocean waters where the light also attenuates quickly [Fig. 3(b)]. This different spectral behavior could be well explained by the calm sea conditions met in those waters, under which conditions there was no significant vertical displacement of the instruments.

Further, one important requirement of the legacy satellite ocean color missions (such as CZCS and MODIS) and future ocean color sensors (e.g. GEO-CAPE and PACE) is to obtain the water-leaving radiance with an accuracy better than 5% for oceanic waters in the blue wavelengths. This has been a great challenge with field measurements due to the many out-of-control factors. The excellent agreement between the measured and theoretically-determined transmittance found here (less than 5% mean error in the 350-600 nm spectral domain) (Table 3) further suggests the skylight-blocked approach is a robust setup to directly measure $L_w(0^+)$ in the field.

Acknowledgments

This study is funded by the National Aeronautic and Space Administration (NASA) Ocean Biology and Biogeochemistry and Water and Energy Cycle Programs and the National Oceanic and Atmospheric Administration (NOAA) JPSS VIIRS Ocean Color Cal/Val Project. Field measurements in Puerto Rico were partially supported by NOAA CREST Grant # NA06OAR480162. We thank Dr. Giuseppe Zibordi for assistance in the field campaign. Three anonymous reviewers are thanked for their comments and suggestions.

#234268 - $15.00 USD Received 10 Feb 2015; revised 3 Apr 2015; accepted 23 Apr 2015; published 27 Apr 2015